The Plant Cell, Vol. 24: 4252–4265, October 2012, www.plantcell.org

Bidirectional Secretions from Glandular Trichomes of Pyrethrum Enable Immunization of Seedlings[W]

Aldana M. Ramirez,[a,b,c] Geert Stoopen,[a] Tila R. Menzel,[a,b] Rieta Gols,[b] Harro J. Bouwmeester,[c] Marcel Dicke,[b] and Maarten A. Jongsma[a,1]

[a] Plant Research International, Wageningen University and Research Centre, 6708 PB Wageningen, The Netherlands
[b] Laboratory of Entomology, Wageningen University, 6708 PB Wageningen, The Netherlands
[c] Laboratory of Plant Physiology, Wageningen University, 6708 PB Wageningen, The Netherlands

Glandular trichomes are currently known only to store mono- and sesquiterpene compounds in the subcuticular cavity just above the apical cells of trichomes or emit them into the headspace. We demonstrate that basipetal secretions can also occur, by addressing the organization of the biosynthesis and storage of pyrethrins in pyrethrum (*Tanacetum cinerariifolium*) flowers. Pyrethrum produces a diverse array of pyrethrins and sesquiterpene lactones for plant defense. The highest concentrations accumulate in the flower achenes, which are densely covered by glandular trichomes. The trichomes of mature achenes contain sesquiterpene lactones and other secondary metabolites, but no pyrethrins. However, during achene maturation, the key pyrethrin biosynthetic pathway enzyme chrysanthemyl diphosphate synthase is expressed only in glandular trichomes. We show evidence that chrysanthemic acid is translocated from trichomes to pericarp, where it is esterified into pyrethrins that accumulate in intercellular spaces. During seed maturation, pyrethrins are then absorbed by the embryo, and during seed germination, the embryo-stored pyrethrins are recruited by seedling tissues, which, for lack of trichomes, cannot produce pyrethrins themselves. The findings demonstrate that plant glandular trichomes can selectively secrete in a basipetal direction monoterpenoids, which can reach distant tissues, participate in chemical conversions, and immunize seedlings against insects and fungi.

INTRODUCTION

The perennial herbaceous plant *Tanacetum cinerariifolium* (Asteraceae), also known as pyrethrum, is an economically important crop used for the production of a group of potent insecticidal secondary metabolites collectively called pyrethrins (Casida and Quistad, 1995). Despite the economic significance of pyrethrins, many aspects of their biosynthesis and cellular localization are poorly understood. Pyrethrins occur throughout the aerial parts of the plant but are concentrated in the dry fruits (achenes, fruits containing a single seed) at levels that are 10 to 20 times higher than in leaves (Head, 1966). Both the biseriate, capitate glandular trichomes on the outside of achenes and secretory duct-like structures inside the pericarp of achenes have been suggested to be involved in the production and storage of pyrethrins (Chandler, 1951, 1954). Evidence supporting a role for trichomes is the reported association of a pyrethrin-void mutant line with the absence of both pyrethrin-containing ducts and trichomes (Chandler, 1951) and the correlation between pyrethrin content and the number and development of trichomes on ovaries and leaves (Zito et al., 1983; Crombie, 1995). However, direct evidence for the role of trichomes in pyrethrin biosynthesis and storage is lacking.

[1] Address correspondence to maarten.jongsma@wur.nl.
The author responsible for distribution of materials integral to the findings presented in this article in accordance with the policy described in the Instructions for Authors (www.plantcell.org) is: Maarten A. Jongsma (maarten.jongsma@wur.nl).
[W] Online version contains Web-only data.
www.plantcell.org/cgi/doi/10.1105/tpc.112.105031

A typical pyrethrum flower hexane extract consists of six pyrethrin esters: pyrethrin I (PI), cinerin I, jasmolin I, and pyrethrin II, cinerin II, and jasmolin II (Figure 1) (Crombie, 1995), and a variety of other compounds, including waxes, fatty acids, glycerides, carotenoids, and terpenoids, such as *E*-β-farnesene, γ-cadinene, and sesquiterpene lactones (Maciver, 1995). The pyrethrin esters derive from the condensation of a terpenoid acid and an oxylipin pathway-derived alcohol moiety (Matsuda et al., 2005). The terpenoid acids are irregular monoterpenoids with c1′-2-3 linkages between two dimethylallyl units and can be either chrysanthemic acid (CA; Type I) or pyrethric acid (Type II) (see Supplemental Figure 1 online) (Rivera et al., 2001). The alcohol part consists of pyrethrolone, cinerolone, or jasmolone, which are linolenic acid derivatives and share the biosynthetic pathway with jasmonic acid. The formation of chrysanthemyl diphosphate from two molecules of dimethylallyl diphosphate (DMAPP) by chrysanthemyl diphosphate synthase (CDS) represents the first dedicated step in the biosynthesis of pyrethrins and was demonstrated in pyrethrum and *Artemisia tridentata* (Rivera et al., 2001; Hemmerlin et al., 2003). *CDS* evolved relatively recently after a gene duplication from an ancestral farnesyl diphosphate synthase (*FDS*) gene. In that process, it acquired a plastid targeting signal, which enabled access to DMAPP derived from the methylerythritol-4-phosphate (MEP) pathway (Rivera et al., 2001; Thulasiram et al., 2007). Very recently, a second dedicated enzyme, *T. cinerariifolium* GDSL Lipase-like Protein (*GLIP*), responsible for the specific esterification of chrysanthemoyl-CoA thioester and pyrethrolone to form pyrethrin I, was discovered (Kikuta et al., 2012).

Generally, glandular trichomes are involved in the synthesis, storage, and emission of a broad array of secondary metabolites

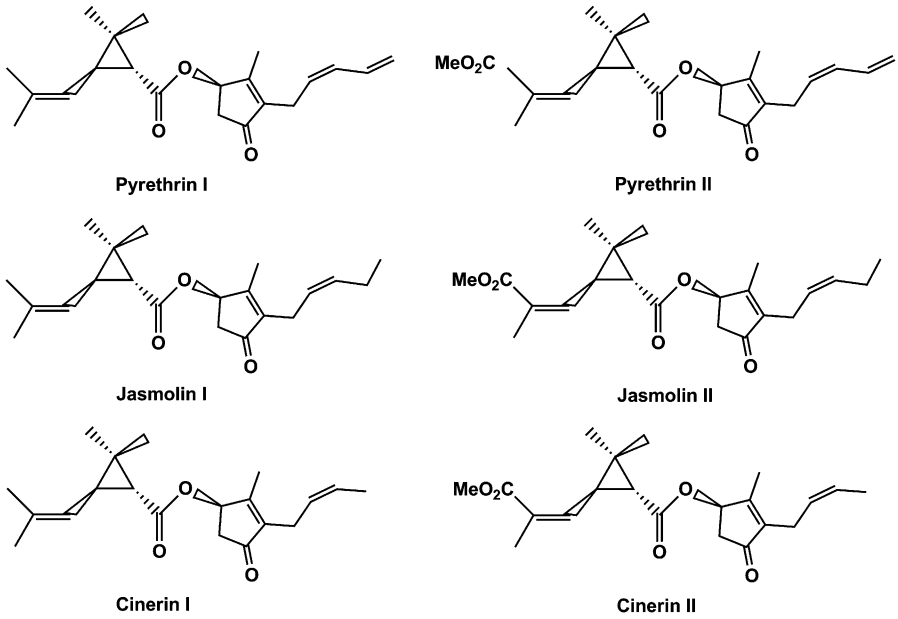

Figure 1. Structures of Natural Pyrethrins.

(Werker, 2000). In the *Asteraceae* family, glandular trichomes are particularly rich in sesquiterpenoids (Seaman et al., 1980; Heinrich et al., 2002; Göpfert et al., 2005; Bertea et al., 2006). Indeed, apart from pyrethrins, pyrethrum extracts also contain a variety of sesquiterpene lactones (STLs), such as pyrethrosin (chrysanthin) (Barton and Demayo, 1957; Barton et al., 1960), chrysanin, dihydro-β-cyclopyrethrosin, chrysanolide, and β-cyclopyrethrosin (Doskotch and Elferaly, 1969; Doskotch et al., 1971). STLs are generally characterized by a five-membered α-methylene-γ-lactone ring. Many also contain additional oxidized positions, and they may be conjugated to glycosides (Sashida et al., 1983; de Kraker et al., 1998). Like pyrethrins, STLs have been implicated in plant defense. They protect plants against insects, pathogenic bacteria, and fungi or play allelopathic roles (Kumar et al., 2005). STLs were specifically described to be cytotoxic (Abeysekera et al., 1985), antibacterial (Picman and Towers, 1983), antifungal (Picman, 1983), phytotoxic (Iino et al., 1972), and germination inhibitors (Sashida et al., 1983).

The terpenoids produced in biseriate capitate glandular trichomes are thus far known to be secreted toward the apical side, resulting in a droplet of secondary metabolites in an extracellular cavity covered by a thick cuticular membrane (Duke and Paul, 1993; Fahn, 2000; Kutchan, 2005). The secretion of metabolites in a basipetal direction, across the epidermis, has not been described. In this article, we investigate the role of pyrethrum trichomes in the biosynthesis and secretion of precursors of pyrethrins and of STLs. We identify the sites of biosynthesis, storage, and deployment of both compounds by chemical, transcriptional, and enzymatic analyses in achene trichomes, pericarp tissues, and seedlings. The potential unknown ecological roles of these compounds are investigated by following their fate in germinating seeds and evaluating their effects against herbivorous insects and a seedling pathogen.

RESULTS

Localization of Oil-Like Substances in Pyrethrum Achenes by Cryo-Scanning Electron Microscopy

To obtain structural information on the localization of oil-like substances in pyrethrum achenes, cryo-scanning electron microscopy images of surface and cross sections of the achenes of disk florets from different flower developmental stages were prepared. Glandular trichomes occurred mainly in four out of five indentations between five ribs in the longitudinal direction of the seed (Figures 2A and 2B), in a density of 650 ± 15 glands per achene for the genotype we evaluated. On the basis of surface density, mature achenes had a sixfold higher glandular trichome density (74 ± 6 trichomes/mm^2) than the combined abaxial and adaxial sides of leaves (12 ± 2 trichomes/mm^2). Biseriate capitate glandular trichomes consisted of a layer of two juxtaposed basal cells (Figure 2C, bc), a layer of two stalk cells (Figure 2C, stc), and three layers of two head or secretory cells (Figure 2C, sec). Cross sections of the glandular trichomes showed that the two cell pairs below the apical cell pair contained chloroplasts, as visible in Figure 2C (arrows), but the apical cells did not. Each trichome was covered with a sac-like cuticular membrane that seemed to adhere firmly to young trichomes but inflate as it filled with oil after opening of the corolla (Figure 2C, Os). Transverse sections of the ovaries of open disc florets with fully developed embryos (prior to desiccation) showed similar oil-like substances as in the trichomes were present in, sometimes air-filled, intercellular spaces of the pericarp surrounding the developing embryo, as well as in the space immediately contacting the epidermis of the cotyledonary tissue of the embryo (Figure 2D, arrows). However, at this immature stage, none were found in the dense cell tissue of the embryo itself.

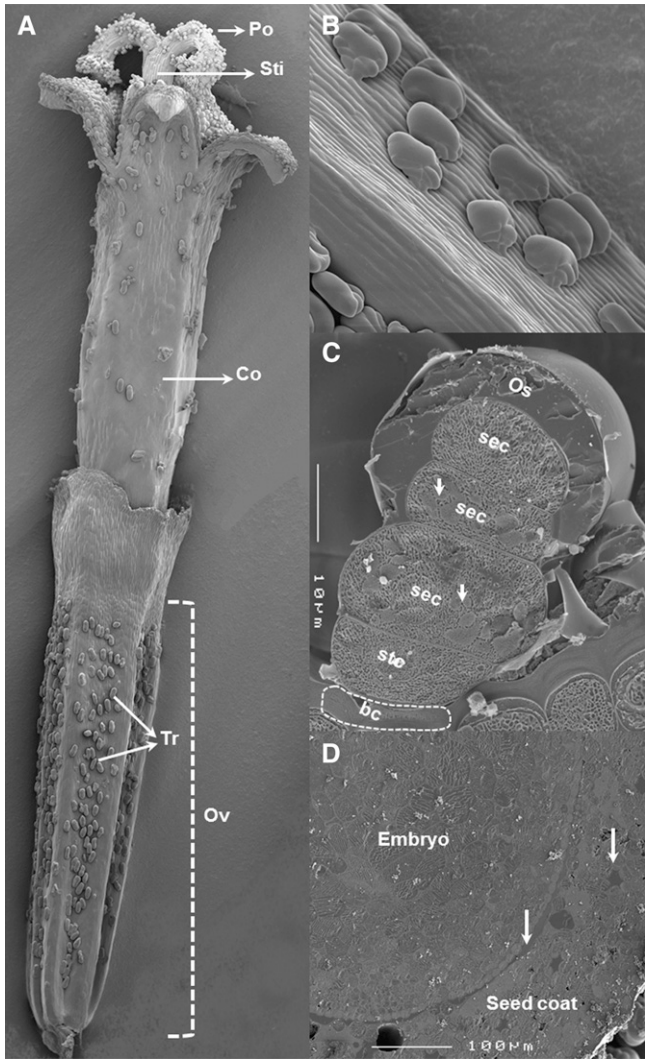

Figure 2. Localization and Morphology of Pyrethrin Stores and Pyrethrum Glandular Trichomes.

(A) Cryo-scanning electron microscopy image of a complete disk floret showing the highest density of glandular trichomes in the indentations between the ribs of the ovary.
(B) Closer view of trichomes.
(C) Side section of a fully developed trichome indicating the location of basal and stalk cells and the presumed secretory cells and the oil sac.
(D) Perpendicular section of a disk floret showing the oil in the intercellular space between the embryo and the seed coat and in the intercellular space of cells (arrows).
bc, basal cell; Co, corolla; Os, oil sac; Ov, ovary; Po, pollen; sec, secretory cell; stc, stalk cell; Sti, stigma; Tr, trichome.

Pyrethrum Glandular Trichomes Store STLs but Not Pyrethrins

To identify the content of glandular trichomes, we analyzed, by gas chromatography–mass spectrometry (GC-MS) and gas chromatography–flame ionization detection (GC-FID), chloroform extracts of (1) complete achenes, (2) trichomes from achenes (using chloroform dipping; see Methods), and (3) achenes after removal of trichome content using chloroform dipping. The GC-MS profiles obtained from trichomes and achenes after chloroform dipping were completely different (Figure 3). The achene content remaining after chloroform dipping consisted mainly of the six pyrethrin esters cinerin I, jasmolin I, PI, cinerin II, jasmolin II, and pyrethrin II (Figure 3B, peaks 1 to 6, respectively) and the thermally induced isoform of PI (Figure 3B, peak 3a) (Goldberg et al., 1965) at an average total concentration of 46.9 ± 3.1 μg/mg (GC-MS) or 65.4 ± 4.6 μg/mg (GC-FID) determination (one seed ~1 mg). The profile obtained for seed trichomes included compounds (A to J) at an average total concentration of 10.9 ± 1.0 μg/mg (GC-MS) or 6.2 ± 1.3 μg/mg (GC-FID) per seed. Comparison of the mass spectrum of each trichome constituent with the NIST library resulted in a list of putative identities, which are summarized in Supplemental Table 1 online. Based on previous characterizations of pyrethrum extracts, dihydro-β-cyclopyrethrosin (Figure 3C, peak F; Kovat's index, 2454) and β-cyclopyrethrosin (Figure 3C, peak M; Kovat's index, 2683) could be assigned, whereas the others require further analysis to determine their exact STL identity. Complete achene extracts yielded a quantitative combination of what was detected in chloroform-dipped achenes and in the chloroform that was used for the dipping (Figure 3A). This demonstrates that chloroform dip extraction was very effective in removing all chloroform-soluble contents from the trichomes without extracting the seed interior. Microscopy examination of vegetative tissues showed that glandular trichomes were present on both sides of the surface of leaves but not on seedling cotyledons. To obtain further information on their chemical composition, the content of leaf trichomes was extracted by chloroform dip as well and compared with the whole ground leaf before and after dipping. We confirmed that pyrethrins also in leaves were confined to the leaf interior (Figure 3E), that the leaf trichomes did not contain pyrethrin esters (Figure 3F), and that leaf trichomes contained the two major STLs of the seed trichomes (Figure 3F, peaks C and E) but lacked the others (Figures 3F and 3C). Seedling extracts (no true leaves) did not contain any STLs but were high in pyrethrin content (Table 1, column 4; Figure 6, peak E).

Pyrethrin Biosynthesis Gene *CDS* Is Expressed in Trichomes, and Pyrethrin Esterification Enzyme *GLIP* Is Expressed in the Pericarp

Having established that pyrethrins, unlike STLs, are not stored in the glandular trichomes, we first investigated the expression of pyrethrin and sesquiterpene biosynthetic genes across different flower stages in relation to the accumulation of the product. As described above, *CDS* catalyzes the formation of the unique monoterpene precursor of pyrethrins, chrysanthemyl diphosphate, whereas farnesyl diphosphate synthase 1 (FDS1) catalyzes the biosynthesis of the sesquiterpene precursor farnesyl diphosphate. GLIP, a GDSL lipase-like protein, was recently reported to catalyze esterification of terpene acids and lipid alcohol substrates into pyrethrins (Kikuta et al., 2012). The expression patterns of *CDS*, *FDS1*, and *GLIP* were analyzed by quantitative RT-PCR and normalized to the *GAPDH* reference gene (see Supplemental Table 2 online). Figure 4 shows that the pyrethrin content of flower stages S1 to S7 (bud to overblown) correlated with the gene expression of both *CDS* and *GLIP*. Fifty

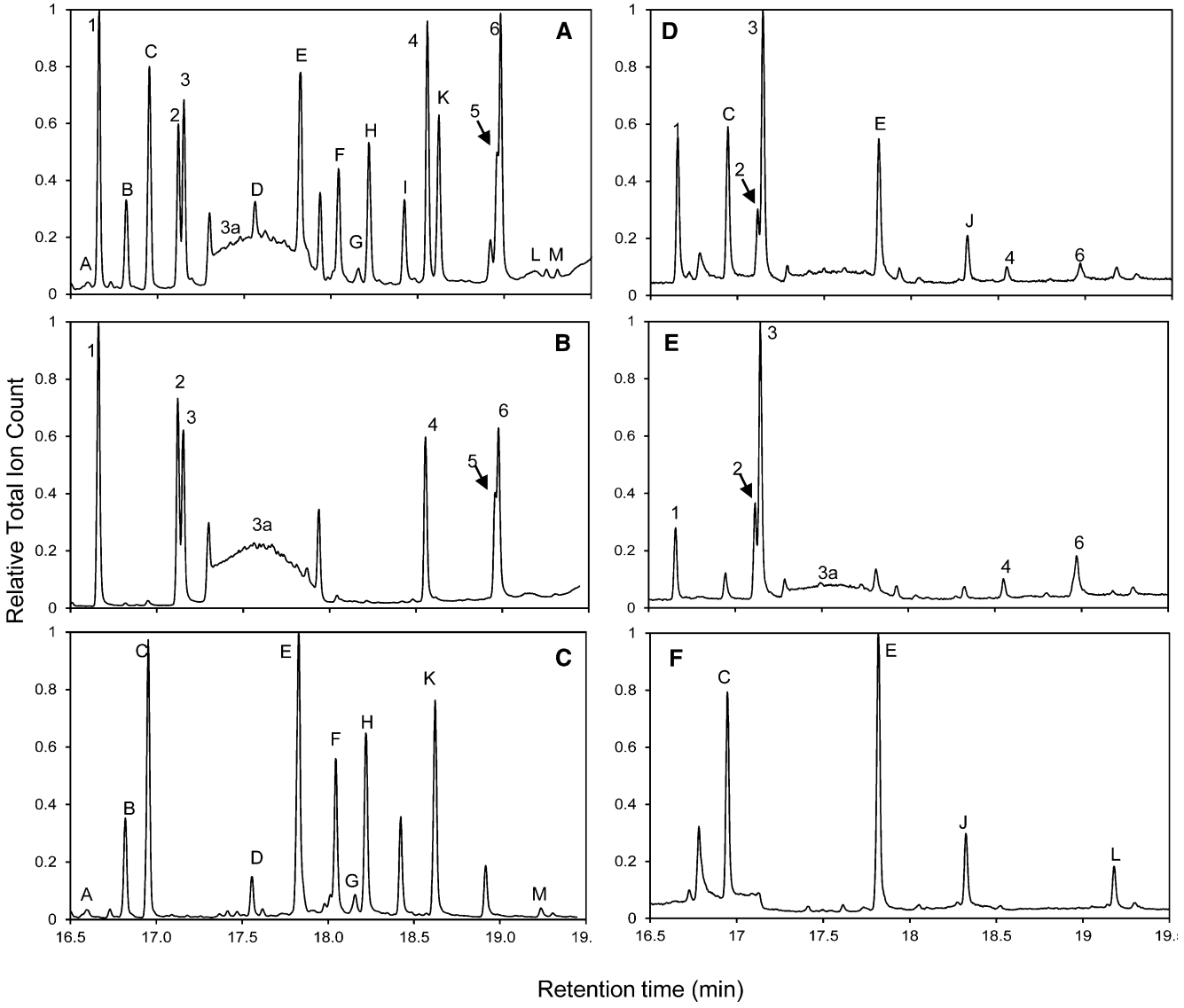

Figure 3. GC-MS Analysis of Pyrethrum Seed and Leaf Oil Constituents.

Chloroform extracts of complete seeds, including trichomes **(A)**, seed contents after trichome extraction **(B)**, contents of seed glandular trichomes only **(C)**, complete young leaves including trichomes **(D)**, leaf contents after trichome extraction **(E)**, and contents of young leaf glandular trichomes **(F)**. The major pyrethrin components identified by mass spectrometry are labeled by numbers: 1, cinerin I; 2, jasmolin I; 3, PI; 4, cinerin II; 5, jasmolin II; 6, pyrethrin II; and the major STLs by letters A to M (see Supplemental Table 1 online for GCMS identification details).

percent of pyrethrins were already produced before the first disc florets opened (stage 2) at a point where embryos were not yet formed, corresponding to the peak of transcription of both *CDS* and *GLIP*.

In a next step, we wanted to know whether pyrethrin biosynthesis occurs in trichomes or the pericarp. To that end, trichomes, ovaries, and ovaries from which trichomes had been largely removed were isolated from stage 3 flowers. The efficiency of removing trichomes from the ovaries was 85%, as established using the STL compound E (exclusively present in trichomes) as an internal standard. Expression of *CDS* in ovaries with trichomes was 5.9% of the expression in trichomes alone, and removing 85% of the trichomes further reduced *CDS* expression in the ovaries by 76% (1.4% of trichomes). This correlation suggested that virtually all *CDS* expression observed in ovaries was derived from the trichomes (Figure 5A). This was supported by the finding that *CDS* was not expressed at all in seedlings at the cotyledon stage, which do not have any trichomes (Figure 6B; microscopy analysis not shown). To verify these observations at the enzyme level, we performed CDS enzyme assays on crude protein extracts of seedlings, ovaries with trichomes, ovaries with trichomes partially removed, and trichomes alone. Except for the seedlings, all of these tissues showed background chrysanthemol

Table 1. Specific Chrysanthemyl Diphosphate Synthase Activity in Crude Protein Extracts of Seedlings, Ovaries, and Trichomes

Tissue[a]	Treatment[b]	COH[c] (area/μL × 1000)	Trichome Lactones[d] (area/μL × 1000)	Protein[e] (ng/μL)	Specific CDS Activity[f] (area/ng)
Seedling	Control	0	0		
	DMAPP	0	0		
	De novo	0 (0%)	(0%)	114	0
Ovaries with trichomes	Control	42 ± 1.6	712 ± 166		
	DMAPP	211 ± 27	537 ± 212		
	De novo	169 (100%)	(100%)	176	193
Ovaries with fewer trichomes	Control	9.2 ± 4.8	229 ± 76		
	DMAPP	70 ± 0.8	178 ± 67		
	De novo	61 (36%)	(32%)	132	93
Glandular trichomes	Control	9.9 ± 4.8	130 ± 62		
	DMAPP	51 ± 18	110 ± 104		
	De novo	41 (24%)	(20%)	2.80	2973

[a]CDS activity was based on extracts of 250 mg tissue. Glandular trichomes were removed from 250 mg ovaries with ~68% efficiency and recovered with ~20% efficiency, column 4.
[b]In the treatments, "De novo" refers to the subtraction of COH content of controls from DMAPP-incubated extracts
[c]COH peak areas of specific mass 123 are given (±SD, $n = 3$). Relative total CDS activity is given in parentheses.
[d]Trichome lactones are peak areas of specific mass 83 (±SD, $n = 3$) of STL compound E and representative of trichome numbers in various tissue preparations. Calculated relative trichome numbers are given in parentheses, averaged for control and DMAPP.
[e]Protein concentrations are given per tissue type and are the same per treatment.
[f]Specific CDS activity is only given for de novo–produced chrysanthemyl.

(COH) even without the addition of DMAPP. However, its concentration increased five to eight times in the presence of DMAPP and subsequent phosphatase treatment (Table 1, control versus DMAPP), showing that most of the COH originated from CDS enzyme activity. These de novo CDS enzyme activities closely matched the estimated trichome numbers in the different tissue preparations as calculated from the STL (peak E) content. Comparing the specific CDS activity per unit protein, we observed a 30-fold difference between trichomes and ovaries with less trichomes, but the activity in the latter preparation also obviously was derived from the remaining trichomes, and the actual difference in specific activity between pericarp and trichomes was therefore much higher (Table 1). Furthermore, just as in the transcript analysis, CDS activity was not detected in seedlings, which are devoid of trichomes.

The expression of *GLIP* was surprisingly different from that of *CDS*. Its expression in the ovaries with trichomes was 14-fold higher than in trichomes alone, and removing 85% of the trichomes further increased *GLIP* expression to a 39-fold difference with trichomes (Figure 5A). Also, in seedlings, *GLIP* was expressed at levels similar to leaves, which was unexpected because in seedlings there was no *CDS* gene expression or CDS enzyme activity at all (Figure 6B).

The expression of *FDS1*, involved in sesquiterpene and other isoprenoid precursor production, was intermediate between *CDS* and *GLIP*. Expression in ovaries with trichomes was 18% of the expression in trichomes (fivefold lower), and removing 85% of the trichomes reduced *FDS1* expression in the ovaries by 57% compared with the ovaries with trichomes, resulting in 13-fold lower *FDS1* expression compared with trichomes (Figure 5A). *FDS1* was expressed equally high in seedlings compared with leaf tissues (Figure 6B). Just like *GLIP*, *FDS1* was also expressed in nontrichome tissues, although at 8- to 13-fold lower levels, which is in line with its broader role in plant metabolism.

CA Is Exported from Trichomes in a Basipetal Direction to the Pericarp

The transcript and enzymatic results strongly suggest that biosynthesis of the terpene precursors of pyrethrins by CDS occurs in the trichomes but that the esterification step most likely occurs in the pericarp. This implies that there should be transport of CDS products from the trichomes to the pericarp. We hypothesized that biosynthetically active trichome tissues should contain transient, low concentrations of terpene precursors and possibly also pyrethrins if trichomes were to perform that step as well, despite the low transcript levels of *GLIP*. To analyze this, the chemical composition of trichomes (knocked off in liquid nitrogen) derived from biosynthetically active ovaries (stage 3, just after opening of the flower) was compared with the chemical composition of intact ovaries (see Supplemental Table 3 online) and ovaries from which the trichomes had been removed (Figure 5B). After normalization against trichome-derived peak E, which was specific for trichomes, it was established that COH was exclusively present in the trichomes (Figure 5B, COH, 178% ± 64% was not significantly different from the trichome-specific peak E distribution, 100% ± 20%; see Supplemental Table 3 online). COH is the primary product of CDS after dephosphorylation, and this finding directly supports our hypothesis that all enzyme activity is contained in the trichomes. In a next step, COH is oxidized into CA, but trichomes only contained 25% ± 5% CA, with the remaining 75% being in the pericarp. Apparently, CA is exported from the trichomes to serve as a substrate for GLIP, which is localized in the pericarp to make pyrethrins. Indeed, the relative content of

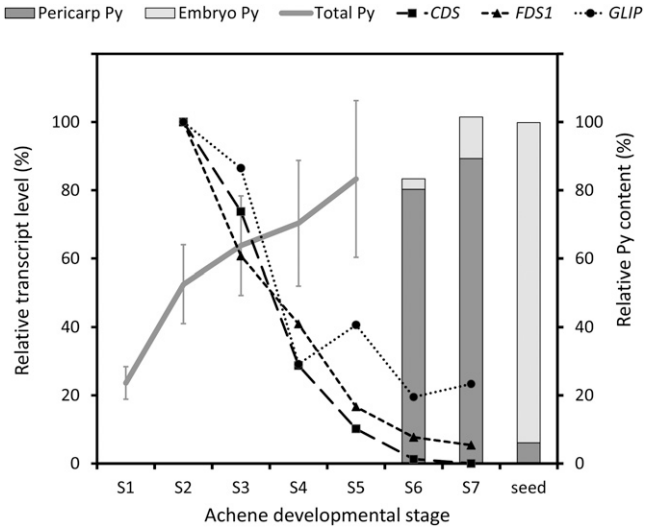

Figure 4. Correlation of Pyrethrin Product Accumulation and Gene Expression across All Stages of Achene Development.

Pyrethrin (Py) content was measured in whole flowers of stages 1 to 5 (S1 to S5). For the final stages 6 and 7, dry seeds, embryos, and pericarps were microdissected and separately examined for pyrethrin content. Peak areas were determined using specific masses 123 or 133. For the graph, stages 5 and 6 were matched to have the same relative content, but stage 6 will be somewhat higher. Transcript levels of *CDS*, *FDS1*, and *GLIP* were measured in dissected ovaries stages 2 to 7 and normalized against *GAPDH*. All data were determined in triplicate. SE error bars were left out for most data for better visualization.

pyrethrins was extremely low in trichomes (0.55%), and there was no significant difference in concentration between these esters relative to the complement in the pericarp from which the trichomes were isolated.

In conclusion, these experiments show that the terpene precursor of pyrethrin biosynthesis, CA, is synthesized via COH in the trichomes and is then transported to the pericarp, where it is used by the pericarp-specific GLIP to synthesize pyrethrins (Figure 7).

Pyrethrins Accumulating in Pericarp Tissues Are Absorbed by the Embryo and Ultimately Are Found in Seedlings

Pyrethrins appear to accumulate in the intercellular space of the pericarp surrounding the developing embryo based on the observation of electron-dense areas, suggestive of lipophilic metabolites in Figure 2C and our finding in Figure 3B that pyrethrins represented the major class of compounds extractable by organic solvents from pericarp and embryo tissues. To obtain better evidence on the localization of pyrethrins during seed maturation and desiccation, we separated and analyzed the pyrethrin content of embryo and pericarp tissues of flower stages 6 and 7 and mature seeds (Figure 4). The content of pyrethrins decreased in pericarp tissues from stage 7 to mature seeds, while it increased at the same rate in the embryo during that phase. These observations prompted us to investigate what happened after seed germination. GC-MS analysis of the chemical composition of seeds, husks, and seedlings showed that all pyrethrin esters originally present in the achene (Figure 6A, seeds), but only 4% of CA, were present in seedling extracts after germination. Only 7 to 24% of these esters and CA remained in the husk after the seedling had emerged. Dipping of the seedlings in chloroform to wash off any compounds present on the surface resulted in 4 to 10% of pyrethrins (Figure 6A). The STLs, on the other hand, did not migrate to the seedling, as they were not detected in any seedling tissue after germination, and only a small amount remained in the husk.

To distinguish whether pyrethrins in the seedlings were synthesized de novo or recruited from the embryo, the expression of *CDS*, *GLIP*, and *FDS1* was analyzed in seedlings. *FDS1* and *GLIP* were expressed in leaves and seedlings, whereas *CDS* was not expressed at all in seedlings (which do not have trichomes) at both the RNA and enzyme level, while it was highly active in the true leaves of older seedlings, which are rich in

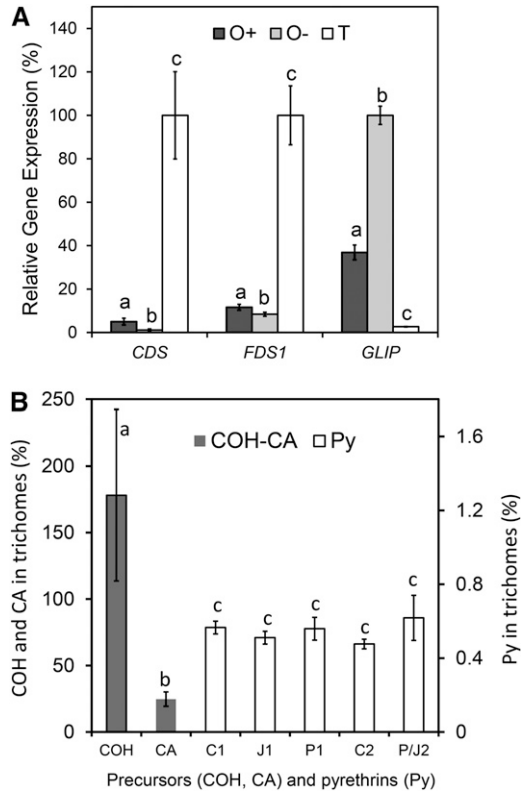

Figure 5. The Terpene Precursors of Pyrethrin Biosynthesis Are Synthesized in Trichomes and Transported to the Pericarp.

(A) Relative gene expression of *CDS*, *FDS1*, and *GLIP* in ovaries with trichomes (O+), ovaries with 85% fewer trichomes (O-), and isolated glandular trichomes (T) after normalization against *GAPDH* expression. Lowercase letters indicate significant differences for that gene relative to the other tissues ($P < 0.05$).

(B) The relative content of precursors COH and CA, and pyrethrins (Py; right *y* axis) that could be traced to be specifically contained in trichomes and not in pericarp (see Supplemental Tables 2 and 3 online; peak areas of specific masses were integrated per compound). Lowercase letters indicate significant differences. Error bars represent SE ($n = 3$).

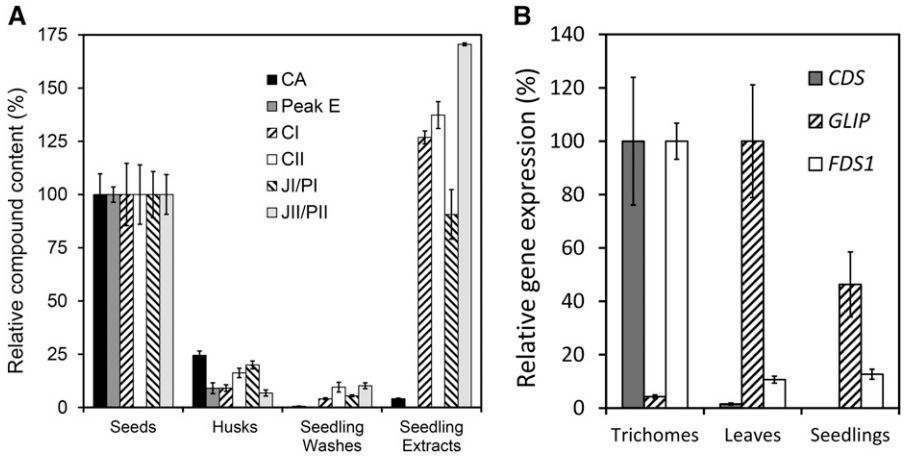

Figure 6. Pyrethrins from Embryos Protect Seedlings.

(A) Relative peak areas (specific masses) of CA, STL peak E, and the different pyrethrin esters in husk extracts, seedling washes, and seedling extracts relative to intact seeds (100%).

(B) Relative gene expression of *CDS*, *GLIP*, and *FDS1* in trichomes, leaves, and seedlings after normalization with *GAPDH*. All data were determined in triplicate. Error bars represent SE. See Supplemental Tables 2 and 4 online for supporting data.

glandular trichomes (Figure 6B, Table 1). The lower concentrations of CA and STLs may be explained by loss of trichomes during seed germination, metabolization, or release to the medium. In the case of CA, it may be that the GLIP activity in the cotyledons used the remaining maternal CA to synthesize new pyrethrins, which could explain the relatively higher levels compared with the original seeds. These combined results demonstrate that pyrethrins are translocated from the pericarp to inner tissues of the maturing embryo and finally to inner tissues of the germinating seedling (Figure 7).

Pyrethrum Seed Trichome Content Is Insect Antifeedant and Pyrethrins Have Antifungal Properties

The association of pyrethrins and trichome STLs with leaves and germinating seedlings suggests that they may have multiple roles in plant defense. The effects of pyrethrins against insect herbivores have been published (Casida and Quistad, 1995). To learn the potential effects of the STL trichome content on insect herbivores, we assayed its effects on a specialist (*Pieris brassicae*) and a generalist (*Mamestra brassicae*) caterpillar. At the highest tested dose (300 ng/mm^2), the trichome oil showed deterrent activity against both the specialist (Figure 8A) and the generalist (Figure 8B) caterpillars. At a lower concentration (60 ng/mm^2), only the specialist caterpillar was affected (Figure 8A).

Pyrethrins and trichome oil may possess antimicrobial activities that could potentially explain their high concentrations on seeds and seedlings. The fungal pathogen *Rhizoctonia solani* primarily attacks belowground plant parts, such as the seeds, hypocotyls, and roots, but can also infect aboveground plant parts, such as pods, fruits, leaves, and stems. It is an important pathogen of pyrethrum causing root rot and wilting of the plants (Alam et al., 2006). The most common symptom of *Rhizoctonia* disease is referred to as "damping off" characterized by nongermination of severely infected seeds, whereas infected seedlings can be killed either before or after they emerge from the soil. To test the toxicity of trichome oil and pyrethrins to this fungus, we assayed radial growth at two concentrations (70 and 220 μg/mL). At a concentration of 220 μg/mL, pyrethrins slowed radial growth of *R. solani* by 50%, whereas trichome oils reduced growth by 30%. After threefold dilution, the trichome oil was ineffective, whereas pyrethrins still inhibited fungal growth significantly by 38% (Figure 8C). The average weight of seedlings was 3.5 mg, and one seed contained 45 to 65 μg pyrethrins. The concentration pyrethrins in the seedlings is thus ~1.5 to 2% (w/fresh weight), which is ~70- to 100-fold higher than the concentration, yielding 50% inhibition of *R. solani* radial growth in vitro. Therefore, pyrethrins may prevent or inhibit germination of spores of pathogens and hence contribute to seedling survival.

DISCUSSION

Terpene Metabolites of Pyrethrum Seed Trichomes Are Selectively Transported in Apical and Basipetal Directions

The current state of the art is that glandular trichomes store mono- and sesquiterpene compounds in the subcuticular cavity just above the apical cells or emit them into the headspace (Fahn, 2000; Kutchan, 2005). Here, we show that specific terpenoid metabolites produced in glandular trichomes can also be selectively secreted and sequestered in a basipetal direction. More specifically, we demonstrate that trichomes selectively secrete sesquiterpenoids in the apical direction and monoterpenoids in the basipetal direction (Figure 7).

Previous research by Brodelius and coworkers (Olsson et al., 2009; Olofsson et al., 2012) provided evidence that sesquiterpene and monoterpene production may to some extent be divided between apical and subapical cells of *Artemisia annua* glandular trichomes. The evidence so far suggests that artemisinin biosynthesis genes are expressed in both layers (Olofsson

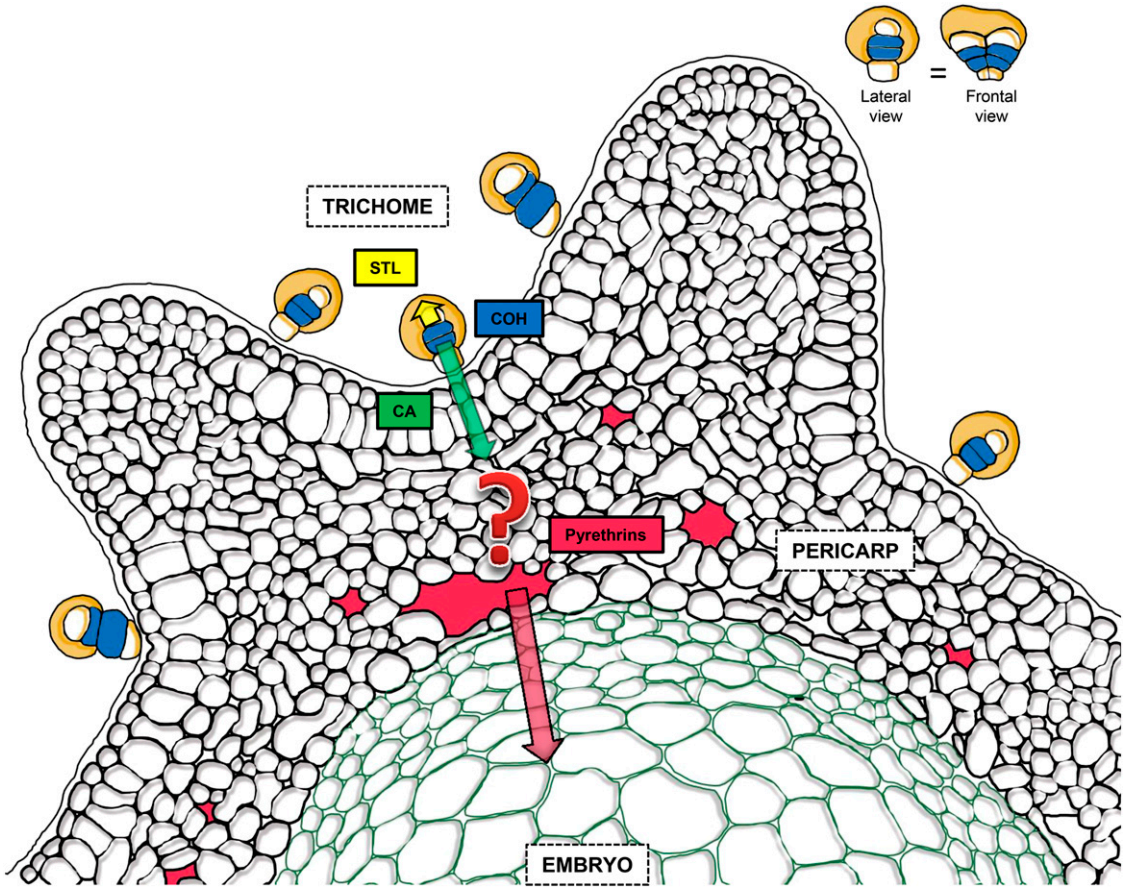

Figure 7. Proposed Model for Bidirectional Secretions from Glandular Trichomes of Pyrethrum That Enable Immunization of Seedlings.

STLs are secreted in an apical direction from the white apical cells to the subcuticular space (yellow). In the blue subapical cells, the terpene substrate of pyrethrin biosynthesis is synthesized. This leads to the formation of chrysanthemyl diphosphate and COH. COH is oxidized into CA and then exported to the pericarp (green arrow). The enzyme GLIP, which forms pyrethrin esters by joining chrysanthmoyl-CoA to lipid alcohols, resides in the pericarp and is active in the apoplast according to Kikuta et al. (2012), but the question mark indicates that it is unclear where and how the esterification occurs precisely. Pyrethrins subsequently accumulate in the intercellular spaces of pericarp, surrounding the embryo. During seed maturation, they are absorbed into the embryo. Seeds germinate with high pyrethrin concentrations in the seedlings. Trichomes are a biseriate stack of five paired cells oriented along the groove of the seed. The inset shows the lateral and frontal views of the trichomes for the purpose of clarity. The figure is based on an original cryo-scanning electron microscopy image shown in Supplemental Figure 2 online.

et al., 2012). However, germacrene A synthase (germacrene A is a precursor of STLs in pyrethrum) has been only detected in chloroplast-free apical cells (Olofsson et al., 2012), and 1-deoxy-D-xylulose-5-phosphate reductoisomerase participating in the plastidial MEP pathway and linalool synthase were amplified only from the chloroplast-containing subapical cells (Olsson et al., 2009; Olofsson et al., 2012). *A. annua* trichomes have an additional stalk cell layer compared with pyrethrum glandular trichomes, but otherwise they are phenotypically very similar (Duke and Paul, 1993). Therefore, to understand the mechanism of selective secretion of STLs and pyrethrins, we propose that STLs of pyrethrum are mainly produced in the apical cell layer without chloroplasts, allowing immediate secretion into the subcuticular space, whereas monoterpenoid pyrethrin precursors are produced by the subapical cells with chloroplasts. CDS in pyrethrin biosynthesis is dependent on the MEP pathway (Matsuda et al., 2005) and is localized in chloroplasts (Hemmerlin et al., 2003). Secretion of pyrethrin precursors from these subapical cells may be blocked in the apical direction, resulting in default secretion in a basipetal direction, or, alternatively, there may be an active process involving specific proteins that transport monoterpenoid precursors of pyrethrins in the basipetal direction. Duke and Paul (1993) studied very similar glandular trichomes of *A. annua* and showed by transmission electron microscopy that osmiophilic (=lipid) material is produced profusely by chloroplast-containing subapical cells and is present between plasma membranes and cell walls that do not border the subcuticular space. This supports the contention that the subapical cells of biseriate capitate glandular trichomes from *Asteraceae* are able to secrete osmium-colored products (most likely terpenoids) into the intercellular space, even though it does not prove that basipetal transport occurs.

Further research is needed to confirm this task division of apical and subapical cells in sesquiterpenoid and monoterpenoid

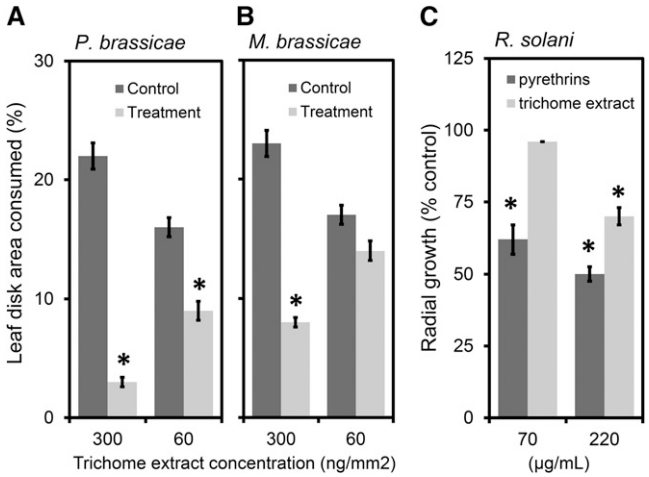

Figure 8. Pyrethrum Seed Trichome Content Is Insect Antifeedant and Pyrethrins Have Antifungal Properties.

(A) and **(B)** Percentage of cabbage leaf disk area consumed by the specialist caterpillar *P. brassicae* **(A)** and the generalist caterpillar *M. brassicae* **(B)** in relation to the surface concentration of trichome extract ($n = 20$).

(C) *R. solani* radial growth reduction given as percentage of ethanol solvent control for two tested concentrations (70 and 220 µg/mL) of trichome compounds and pyrethrin oil ($n = 3$).

Asterisks indicate significant differences between treatment and control ($P < 0.05$; Student's t test). Error bars represent SE.

production and secretion and to understand which transport mechanisms are operating. That work must also answer the question of how GLIP forms pyrethrin esters in the pericarp, from where it recruits the lipid alcohols, and whether this occurs intracellularly or in the apoplast as recently proposed (Kikuta et al., 2012). The C terminus of GLIP ends with the peptide NDEL, which is a well-known endoplasmic reticulum retention signal (He et al., 2004). Therefore, it is possible that this enzyme is in fact retained in the endoplasmic reticulum and that C-terminal green fluorescent protein fusions have resulted in an artifact of secretion into the apoplast (Kikuta et al., 2012).

The biosynthesis of monoterpenoids that do accumulate in trichomes has been described best for peppermint (*Mentha piperita*; Kutchan, 2005). Peppermint accumulates large quantities of monoterpenoids in peltate glandular trichomes, which consist of one basal cell, one stalk cell, eight glandular secretory cells, and a subcuticular oil storage cavity. Trafficking of monoterpenoids occurs between plastid, ER, and mitochondria for several oxidation steps, but like sesquiterpenes, they are stored in the apical subcuticular cavity immediately contacting the secretory cells (Kutchan, 2005). The biosynthesis and transformation of the monoterpene indole alkaloid vinblastine in *Catharanthus roseus* and of several benzylisoquinoline-derived alkaloids in opium poppy (*Papaver somniferum*) are organized differently. There, the biosynthesis does not occur in trichomes and is mediated by secretion and uptake of intermediates among at least three cell types. They move from the internal phloem cells or phloem parenchyma to the epidermis or cells surrounding the laticifers and, for their final modification and storage, to laticifers and idioblasts (Kutchan, 2005). Similar intercellular transport mechanisms of monoterpenoid intermediates may also occur in the biosynthesis of pyrethrins, where it is necessary, for example, that CA is activated first by CoA for GLIP to produce pyrethrins.

Translocation to the intercellular space of leaves and achenes may be an adaptation to accumulate larger pyrethrin quantities or to preserve the bioactivity of these compounds, as pyrethrins are sensitive to UV degradation (Dickinson, 1982; Pieper and Rappaport, 1982). Additionally, the mode of action of pyrethrins depends on physical contact with the insect adult, larva, or embryo (Yang et al., 2012). This may occur more effectively if the toxin is present intercellularly in leaves than when contained in surface glands (Yang et al., 2012). Yet, such a mechanism requires that the surrounding cells are tolerant to these compounds, which at high concentrations is not the case for many terpenoids (Duke et al., 1987). Ultimately, however, the significance of a potentially common mechanism of basipetal secretion is that secretory trichomes may participate in the biosynthesis outside the trichomes of compounds that have diverse physiological and defensive functions in the organism.

A Previously Unknown Pathway for Immunizing Seedlings

Our results show that the biosynthesis of pyrethrins starts in the trichomes present on the pericarp of the achenes. Intermediates are exported and used in the pericarp to synthesize pyrethrins, which accumulate in intercellular spaces and are absorbed by the desiccating embryo. Upon germination, these embryo-stored pyrethrins allow the recruitment by seedlings of 100-fold higher concentrations of pyrethrins than normally found in leaves. Cotyledons of pyrethrum completely lack trichomes; thus, without investing itself in defense at all, the uptake by the embryo of pyrethrins from maternal pericarp tissues guarantees a very high level of protection for seedlings (Yang et al., 2012). Similar chemical seedling defenses derived from maternal tissues are based on, for example, phenolics (Hanley and Lamont, 2001), alkaloids (Schaffner et al., 2003), cyanogenic glucosides (Goodger et al., 2002), and glucosinolates (Nour-Eldin and Halkier, 2009). Those secondary metabolites are not formed in trichomes but are also directly stored in cotyledons or endosperm, already at the embryonic stage. Whether pyrethrin absorption is a passive or an active process remains to be investigated, by, for example, testing pyrethrin absorption by embryos of other plant species or by overexpressing putative transporter genes in model organisms, such as yeast or *Xenopus laevis* oocytes (Nour-Eldin and Halkier, 2009).

Roles of Pyrethrins and Trichome Oil in Plant Defense

Secondary metabolites from pyrethrum stored in trichomes or in leaves and seeds provide leaves and seeds with chemical protection against attacking insect herbivores and pathogens and potentially result in fitness benefits (Boege and Marquis, 2005; Elger et al., 2009; Yang et al., 2012). Chemical analysis of pyrethrum leaves and seeds showed that glandular trichomes present on the ovaries have a more complex composition than the glandular trichomes of leaves (Figure 3). The differences may reflect

functional adaptations to specific herbivores and pathogens of leaves and seeds (this report) or even the surrounding competing flora by inhibiting root growth (Sashida et al., 1983). For individual compounds, it was demonstrated that they may have specific biological activities, but these activities cannot yet be generalized to an ecological level, and work is needed to study the effects of genetic variation for these traits (Kumar et al., 2005). Susurluk et al. (2007) showed that STLs from *Tanacetum cadmeum* ssp *cadmeum* aerial plant parts and *Tanacetum corymbosum* ssp *cinereum* flowers are effective antifeedants for the generalist larvae of *Spodoptera littoralis*. Goren et al. (1994) studied the flowers of *Tanacetum argenteum* subsp *argenteum* (*Asteraceae*) and isolated a STL that also showed antifeedant activity against the neonate larvae of *S. littoralis*. We show that the larvae of the *Brassicaceae* specialist *P. brassicae* are more sensitive to trichome oil of pyrethrum than the larvae of the generalist *M. brassicae* that also feed on *Asteraceae*. It is known that specialist herbivores have evolved enzyme systems to detoxify specific plant compounds associated with their specific diet, whereas generalist herbivores are able to produce enzymes to detoxify a wider range of substrates (Krieger et al., 1971; Johnson, 1999; Ratzka et al., 2002). Moreover, particularly *M. brassicae* is known to feed on *Helianthus annuus* (*Asteraceae*), which produces STLs that act as antifeedants for other insects (Mullin et al., 1991). This may explain why *M. brassicae* is less sensitive to the *T. cinerariifolium* trichome compounds applied on cabbage (*Brassica capitata*) leaves than the cabbage specialist *P. brassicae*.

We observed that upon germination, STLs were largely gone from the husks. Presumably, they were dissolved in the germination solution. This argues in favor of roles as antibiotics of soilborne pathogens or inhibitors of root growth of competing flora as was described for pyrethrum lactones at concentrations of 5 ppm (Sashida et al., 1983), whereas on leaves, the antifeedant activity against insects may be more relevant. Surprisingly, pyrethrins were quite potently active to reduce mycelial growth rates of *R. solani*, which causes a major root rot and wilt disease of pyrethrum (Alam et al., 2006). We were unable to test higher concentrations as the ethanol solvent concentration would then become toxic itself. However, in seedling tissues pyrethrins are present at concentrations 100-fold higher than tested by us, and sensitive pathogens might be stopped during the invasion process. The finding that pyrethrins are potent inhibitors of the plant pathogen *R. solani* indeed points to a possible dual role for the high concentrations of pyrethrins in seedlings against both pathogens and insects, and *R. solani* might represent an important selective pressure to maintain high levels of pyrethrins in seeds. The pathogen may still attack other plant parts as the seedling fresh weight concentrations of 1.5-2% (w/w) are ~70–100-fold higher compared with normal concentrations in leaves. Also here, studies are needed to verify these roles, and the existing high genetic variation for the content of pyrethrins in seeds and leaves could be used for this.

In conclusion, glandular trichomes have been widely studied, although so far they are known only to synthesize apically stored or headspace-emitted products. Our findings introduce the need for an extension of the current model of the role and function of glandular trichomes: Trichomes can also secrete products into the intercellular space of subepidermal tissues, and these can even immunize seedlings, allowing roles in tissues that are unable to produce such compounds themselves

METHODS

Plant Material

Tanacetum cinerariifolium seeds were originally obtained from Honghe Senju Biology (Li et al., 2011) and propagated without selection at Plant Research International. Before chemical characterization, seeds were selected by sorting and sieving. Plants were grown in the field in a sandy soil, supplied with a regular fertilizer regime. After an initial flush, plants were flowering continuously from June until the first frost in November. Samples were taken from flowers between the months of June and September.

Cryo-Scanning Electron Microscopy

Whole pyrethrum disc florets and transverse-cut sections of disc florets and embryos isolated from mature seeds were mounted on a brass cylindrical sample holder with TBS (tissue freezing medium; EMS) for imaging of their morphology. All samples were first frozen in liquid nitrogen. To prepare cuttings, florets were placed in a cryo-ultramicrotome (Reichert Ultracut E/FC4D) and cut at a specimen temperature of −100°C with glass and diamond knives (Histo no trough, 8 mm, 45°C; Drukker International). The planed samples and the whole flowers were placed in a dedicated cryo-preparation chamber (CT 1500 HF; Oxford instruments), freeze-dried for 3 min at −90°C at 1×10^{-4} Pa to remove ice contamination from the surface, and subsequently sputtered with a layer of 10-nm platinum. The samples were cryo-transferred into the field emission scanning microscope (JEOL 6300F) on the sample stage at −190°C. All images were recorded digitally (Orion; 6 E.L.I. sprl) at a scan rate of 100 s (full frame) and a size of 2528 × 2030, 8 bit (Elliott, 1964).

Extraction and Analysis of Trichome and Ovary Contents

Seed secretory trichome content was isolated by a brief extraction in 100% chloroform ($CHCl_3$) as described by Duke et al. (1994). One milliliter of solvent was pipetted into a glass vial containing 100 mg of dry seeds and vortexed for 30 s. The solvent was carefully removed from the vial and dehydrated by passing through a Pasteur pipette filled with 2 cm Na_2SO_4. Leaf trichome contents, on the other hand, were isolated by submerging a fresh leaf of known weight in 5 mL $CHCl_3$ for 15 s, followed by a similar dehydration step on sodium sulfate.

To get sufficient trichome oil for the insect bioassays, 5 g of *T. cinerariifolium* seeds were extracted for 30 s in 35 mL $CHCl_3$. After filtering and drying through a 60-mL glass funnel with a glass fritted disc filled with Na_2SO_4, the clear extract was collected in a 250-mL glass evaporation balloon and distilled off with a rotary evaporator (Büchl Rotavapor-R) under vacuum at 150 to 200 mbar. The solution was reduced to 1 mL, split into three equal volumes, and evaporated to complete dryness (10 to 20 mg) under nitrogen flow.

Ovary glandular trichomes were isolated from fresh stage 3 flowers of plant genotype 10, collected from the Plant Research International pyrethrum field. For the isolation of ovaries, ray florets were removed and the composite flower head was cut in half. Corollas of disc florets were abscised at the calyx. The remaining ovaries were then isolated by cutting the achenes from the receptacle and immediate collection in a 2-mL Eppendorf tube filled with liquid nitrogen. Parts of these ovaries (400 mg) were used for trichome isolation. Trichomes were removed from the ovaries with four vortex pulses of 1 min and 1 min cooling rest between pulses in liquid nitrogen. Frozen ovaries were spread on a precooled 150-μm mesh mounted over a precooled 50-mL screw-capped tube. The trichomes that passed through the mesh were collected at the bottom of

the tube and later used for oil extraction with chloroform or RNA isolation with TriPure (Roche). Ovaries without trichomes that remained on the mesh and intact ovaries were collected and stored at −80°C until further use.

Frozen isolated trichomes from plant genotype 10 and from an assorted mixture of genotypes collected from the field were extracted independently with 1 mL of the appropriate solvent, followed by homogenization with a glass potter and 5-min sonication. Intact ovaries, ovaries without trichomes, intact seeds, seeds after chloroform dipping, intact leaves, and seedlings were flash frozen in liquid nitrogen and ground to a fine powder. The content of the tissues (100 mg) was extracted with 1 mL of chloroform, followed by 30 s of vortexing and 5 min of sonication. The extracts were centrifuged for 5 min at 2200*g*, dehydrated using anhydrous Na_2SO_4 and analyzed by GC-MS and GC-FID. Quantification of constituents isolated from trichomes, seeds, and leaves was done by relating peak areas to two reference curves, one of parthenolide for the quantification of STLs, and one of pyrethrum oil for the quantification of pyrethrin esters.

Instrumentation

The GC-MS and GC-FID measurements were conducted on Agilent 7890A gas chromatographs consisting of a 7683 series autosampler, 7683B series injector, and for the mass spectrometer a 5975C inert mass selective detector with triple-axis detector. The detector temperature for the GC-FID was 340°C. Control of the equipment, data acquisition, processing, and management of chromatographic information were performed by the Agilent Enhanced ChemStation E.02.00.493 software. A Zebron ZB-5MS GC13 capillary column (30 m × 0.25 mm i.d. × 0.25-μm film thickness; Phenomenex) with 5-m guard column was employed for both chromatographic analyses. The injector temperature of the GC instruments was set at 250°C. and helium was the carrier gas with a column flow rate of 1.0 mL/min. The injection volume was 1 μL, and samples were injected in splitless mode. The oven temperature was held at 45°C for 2 min and programmed to 300°C at 15°C/min, and the final temperature was held for 4 min. Total run time per sample was 23 min. The mass spectrometer was operated in the electron ionization mode (70 eV) with an ion source temperature of 230°C. The detector was switched on after 4.5 min solvent delay, and the full mass range mode was used for the analyses of the samples with a mass-to-charge ratio range from 45 to 250 atomic mass units, a scan time of 0.2 s, and an interscan delay of 0.1 s. If not described otherwise, samples were prepared in $CHCl_3$ and diluted five times before injection. Constituents of the essential oil were identified by comparing their mass spectra with those of the reference library, the NIST 08 mass spectral database.

Trichome Quantification and Oil Content Determination of Trichomes and Seeds

A number of freshly collected and 1-year-old seeds were placed under a Zeiss fluorescence microscope, and the number of trichomes was counted. The average density of trichomes per seed or seed surface area was determined by scanning images of seeds using the ImageJ software version 1.40 g (National Institute of Health). The average density of trichomes on leaves was determined by counting the number of trichomes on the top and on the bottom of 17-mm-diameter young and old leaf discs.

To estimate the amount of compounds found in trichomes and ovaries by GC-MS and GC-FID, the sum of their respective peak areas was correlated to a standard curve that was generated using different dilutions of a 1-mg/mL parthenolide stock (0×, 2×, 4×, and 6×) and a series of standard curves generated using three different dilutions of pyrethrum oil (0×, 2×, and 4×) containing a mixture of the six pyrethrin esters. Independent calibration curves of the different esters were used to estimate their respective amounts in the samples. Based on the average number of trichomes per seed (650 ± 10 for freshly collected seeds) and the number of seeds used in the extraction (100 seeds per mL), the amount of trichome compounds per seed and per trichome were calculated.

Insect Dual-Choice Assays

Trichome oil constituents were tested for their ability to act as insect deterrents. For insect assays, a chloroform extract of 15 mg trichome components was evaporated and redissolved in 100 μL methanol and diluted in demineralized water with 0.2% (v/v) Tween 80 to the appropriate concentration. Tween 80 was added to suspend insoluble fractions and to facilitate spreading on hydrophobic leaf discs. Control solutions contained methanol, Tween 80, and demineralized water in the same ratios. Leaf discs of 1.7-cm diameter were cut from cabbage (*Brassica oleraceae*) leaves using a cork borer. Six leaf discs were placed in each Petri dish holding a moist filter paper. Ten microliters of either the diluted trichome extract or control solution was pipetted onto a leaf disc in an alternating manner and dispersed with a saturated paintbrush. The Petri dishes were left open for 20 min to allow the leaf discs to dry.

One-fifth instar (L5) caterpillar of the specialist *Pieris brassicae* (Lepidoptera: Pieridae) or the generalist *Mamestra brassicae* (Lepidoptera: Noctuidae) was gently placed in each Petri dish and left to feed for 3 h. Two concentrations, 60 and 300 ng/mm^2, of trichome oleoresin were tested for both *M. brassicae* and *P. brassicae*. Results were scored by scanning the remaining leaf disc areas and analyzing the differences in size using the image software ImageJ. The consumed areas were calculated for treatment and control discs, and a paired Student's *t* test was used to assess differences in consumption of control and pyrethrin-treated leaf discs. Experiments were done in 20 replicates.

Insect Rearing

The insect herbivores were maintained on Brussels sprouts plants (*B. oleracea* var *gemmifera* cv Cyrus) in acclimatized rooms at 20 to 22°C, 50 to 70% relative humidity, and a 16/8-h light/dark photoperiod. *M. brassicae* moths were offered only filter paper as oviposition substrate, without contact with cabbage plants.

Fungal Growth Inhibition Assays

Pyrethrin oil (70% pyrethrins plus 1% butylated hydroxy-toluene; a gift from Honghe Senju Biological) and trichome oil constituents were tested for their ability to inhibit the growth of *Rhizoctonia solani* AG2.2IIIB. For the inhibition assays, the trichome extract (15 mg) and the pyrethrum oil (2 M) was dissolved in 1000 μL ethanol to achieve 50 mM stock solutions (calculated using a molecular weight of 306 of β-cyclopyrethrosin), which were further diluted in R2A agar (BD Difco) to their final concentrations (0, 0.2, 0.6, and 2 mM). Control stock solution contained either ethanol or ethanol/butylated hydroxy-toluene in the same ratios. All media were transferred in 3-mL quantities to six-well microtiter plates. Each well was inoculated with a 5-mm agar disk containing densely grown *R. solani* mycelia and incubated at 20°C in the dark. Growth was monitored over 6 d, and the radial growth was recorded after 1, 2, 3, and 6 d. All tests were performed in triplicate.

Expression Analysis

For RNA extraction, plant tissue was homogenized by adding one precooled grinding ball to each 2-mL Eppendorf containing 50 to 100 mg of frozen plant tissue and using a precooled Mikro-disembrator II (Braun) for 1 min at maximum speed. After careful removal of the beads, RNA was isolated using TriPure (Roche), purified using an RNeasy mini kit (Qiagen), and transcribed into cDNA using TaqMan reverse transcription reagents (Applied Biosystems) according to the manufacturer's instructions.

Quantitative RT-PCR was used to study the expression of *CDS*, *FDS1*, and GDSL lipase (*GLIP*) in cDNA derived from different tissues. Gene-specific primers were design using Beacon Designer Software (TciCDS-F, 5′-CATCTTCTGGACCTCTTCAATGAG-3′; TciCDS-R, 5′-GTACTGAACAATCCGACGGTTAAG-3′; TciFDS1-F, 5′-GGTTGGTATGATTGCTGCGAAC-3′; TciFDS1-R, 5′-TGAACAGGTCAACAAGATCCAC-3′; TciTcGLIP-F, 5′-TTGAGAACTAAGGCAACCTGTAGG-3′; TciTcGLIP-R, 5′-ACCTCTTGTCTGAGCACATATAAGC-3′). The *T. cinerariifolium GAPDH* gene (TciGAPDH-F, 5′-AGACGAGTTTCACAAAGTTG-3′; TciGAPDH-R, 5′-AGGAATCTGAAGGCAAGC-3′) was used for normalization. PCR reactions were prepared in duplicate by mixing in a 500-μL tube, 22.5 μL iQ SYBR green supermix 2x (Bio-Rad Laboratories), 4.5 μL sense primer (3 μM), 4.5 μL antisense primer (3 μM), 11.5 μL deionized water, and 2 μL cDNA template. After vortexing, each mix was distributed into two wells in 20-μL amounts. Quantification of the transcript level was performed in an MyiQ iCycler system (Bio-Rad Laboratories) using a three-step program, which included (1) enzyme activation at 95°C for 3 min, (2) 40 cycles of 95°C for 10 s and 60°C for 30 s, and (3) 95°C for 1 min, from 65 to 95°C for 10 s for dissociation curve analysis. At the end of each run, amplified products were sequenced to verify their identity. Relative expression values were calculated using the efficiency δCt (cycle threshold) method (Livak and Schmittgen, 2001). Average efficiencies of the primers were 2.04 for GAPDH, 2.02 for CDS, 2.08 for FDS1, and 1.91 for GLIP.

Germination Assay

For germination assays, 2 g of *T. cinerariifolium* seeds were placed in a 50-mL polypropylene tube containing 40 mL of tap water and hydroprimed by incubating for 30 min at 27°C in a water bath. After removing the water, seeds were spread onto 8.5-cm-diameter Petri dishes containing moist cotton wool covered with a 9-cm-diameter Whatman Qualitative 1 filter paper. Seeds were incubated in the dark at 4°C for 3 d to synchronize germination. After the cold period, seeds were transferred to room temperature and kept in the dark until germination commenced. Once the first seeds started to germinate, plates were transferred to the light.

Twenty-five fully developed seedlings, 25 husks, and 25 primed seeds were collected in a 2-mL Eppendorf, flash frozen in liquid nitrogen, and ground to a fine powder using a precooled Mikro-disembrator II (Braun) for 1 min at maximum speed. The whole content of the tube was extracted with 1 mL 100% chloroform ($CHCl_3$) and analyzed for pyrethrin content by GC-MS according to the protocol previously described. In order to determine whether pyrethrins are found on the outside of seedlings, prior to being frozen they were subjected to a washing step consisting of dipping the 25 seedlings for 10 s in a 4-mL glass vial containing 2 mL 100% chloroform ($CHCl_3$). The solution was finally brought to 1 mL by evaporating the excess solvent under a nitrogen flow. The procedure was repeated three times (three independent replicates).

Enzymatic Assay

Protein extracts were prepared from seedlings, ovaries with trichomes, ovaries without trichomes, and trichomes. Ovaries without trichomes and trichomes were prepared as previously described. Two hundred fifty grams of frozen material and the trichomes isolated from 250 mg of ovaries were homogenized by adding a precooled grinding ball to each tube and using a precooled Mikro-dismembrator II (Braun) for 3 min at maximum speed. The plant material was resuspended in 500 μL of extraction buffer containing 200 mM Tris-HCl, pH 8, 15 mM β-mercaptoethanol, 1.5% polyvinylpyrrolidone 40, and 30% glycerol. The slurry was incubated at 4°C for 20 min in a rotator. After incubation, samples were centrifuged two times for 10 min at 17,000*g* at 4°C. After the second centrifugation step, the supernatant was immediately used for the enzymatic assay.

For the enzymatic assay, 100 μL of supernatant was incubated with 100 μL of DMAPP (3.3 mM in ethanol) and 400 μL buffer (15 mM MOPSO, pH 7.5, 12.5% [w/w] glycerol, 1 mM ascorbic acid, 0.001% [v/v] Tween20, 1 mM $MgCl_2$, and 2 mM DTT) overnight at 30°C with shaking. Control assays were prepared in the same way but replacing the 100 μL DMAPP by 100 μL ethanol. After incubation, samples were subjected to phosphatase treatment by adding 100 μL Gly (30 mM), 25 μL $ZnCl_2$ (100 mM), and 3.5 μL phosphatase, incubating for 1 h at 37°C. After adding 250 mg NaCl, samples were extracted with 1 mL ethyl acetate. Followed by 5 min centrifugation at 1200*g*, the organic phase was dried using an anhydrous Na_2SO_4 glass-wool plugged column and analyzed on a GC-MS instrument as described before. Protein determination of soluble enzymes was done by Bradford assay (Bio-Rad Laboratories) according to the manufacturer's instructions.

Pyrethrin Content Determination of Pericarp and Embryo

Embryos were separated from the pericarp of ovaries from flower developmental stages 6 and 7. Fifteen frozen ovaries of each stage and 15 fully developed seeds were cut open with the help of a scalpel, and the embryo was carefully separated and removed. Embryos, the remaining pericarp tissues, and intact ovaries or seeds were flash frozen in liquid nitrogen, ground to a fine powder, extracted with 1 mL $CHCl_3$, and analyzed by GC-MS according to the protocol described above. The isolation procedure was repeated three times with the exception of developmental stage 6, from which embryos were still very small and difficult to isolate.

Accession Numbers

Sequence data from this article can be found in the GenBank/EMBL data libraries under the following accession numbers: CDS, JX913536; CLIP, JX913533; FDS1, JX913534; and GADPH, JX913535.

Supplemental Data

The following materials are available in the online version of this article.

Supplemental Figure 1. Biosynthesis of Pyrethrins and Sesquiterpene Lactones.

Supplemental Figure 2. Cryo-Scanning Electron Microscopy Image of a Cross Section of an Achene That Was Used to Draw Figure 7.

Supplemental Table 1. List of Compounds Detected by GC-MS.

Supplemental Table 2. Non-Normalized and Normalized qRT-PCR Results for Four Biosynthetic Genes and the *GAPDH* Gene (Used for Normalization).

Supplemental Table 3. Content of Pyrethrin Biosynthesis-Related Compounds in Ovaries and Trichomes in Terms of Specific Masses and Relative to Ovaries with Fewer Trichomes before and after Normalization with the Content of STL (Measure for Trichome Quantities).

Supplemental Table 4. Peak Areas Based on Specific Masses (Blue Panels) of Chrysanthemic Acid, STL Peak E, and the Different Pyrethrin Esters in Husk Extracts, Seedling Washes, and Seedling Extracts Relative to Intact Seeds (100%, Yellow Panels).

ACKNOWLEDGMENTS

We thank Adriaan van Aelst for making the cryo-scanning electron microscopy images, Léon Westerd, André Gidding, and Frans van Aggelen for providing insects, Joeke Postma for assistance with the fungal inhibition assay, and

Annemarie Dechesne for her assistance with the GC-FID measurements. We also thank Honghe Senju for providing the seeds that made most of this work possible. This research was supported by Top Technology Institute (TTI) Green Genetics (Stichting TTI Groene Genetica) of the Netherlands (Grant 1C001RP).

AUTHOR CONTRIBUTIONS

A.M.R., H.J.B., M.D., R.G., and M.A.J. designed the research. A.M.R., G.S., and T.R.M. performed research. A.M.R., G.S., T.R.M., R.G., and M.A.J. analyzed data. A.M.R. and M.A.J. wrote the article. M.D. and H.J.B. critically read the article.

Received September 11, 2012; revised September 11, 2012; accepted October 8, 2012; published October 26, 2012.

REFERENCES

Abeysekera, B.F., Abramowski, Z., and Towers, G.H.N. (1985). Chromosomal-aberrations caused by sesquiterpene lactones in chinese-hamster ovary cells. Biochem. Syst. Ecol. **13:** 365–369.

Alam, M., Sattar, A., Samad, A., and Khanuja, S.P.S. (2006). A root rot and wilt disease of pyrethrum (*Chrysanthemum cineraefolium*) caused by *Rhizoctonia solani* AG-4 in the north Indian plains. Plant Pathol. **55:** 301.

Barton, D.H.R., Bockman, O.C., and Demayo, P. (1960). Sesquiterpenoids12. Further investigations on the chemistry of pyrethrosin. J. Chem. Soc. 2263–2271.

Barton, D.H.R., and Demayo, P. (1957). Sesquiterpenoids 8. The constitution of pyrethrosin. J. Chem. Soc. 150–158.

Bertea, C.M., Voster, A., Verstappen, F.W.A., Maffei, M., Beekwilder, J., and Bouwmeester, H.J. (2006). Isoprenoid biosynthesis in *Artemisia annua*: Cloning and heterologous expression of a germacrene A synthase from a glandular trichome cDNA library. Arch. Biochem. Biophys. **448:** 3–12.

Boege, K., and Marquis, R.J. (2005). Facing herbivory as you grow up: The ontogeny of resistance in plants. Trends Ecol. Evol. **20:** 441–448.

Casida, J.E., and Quistad, G.B. (1995). Pyrethrum Flowers: Production, Chemistry, Toxicology, and Uses. (New York: Oxford University Press).

Chandler, S. (1951). Botanical aspects of pyrethrum. General consideration; the seat of the active principles. Pyrethrum Post **2:** 1–9.

Chandler, S. (1954). Botanical aspects of pyrethrum: II. Further observations. Pyrethrum Post **3:** 6–11.

Crombie, L. (1995). Chemistry of Pyrethrins. In Pyrethrum Flowers: Production, Chemistry, Toxicology, and Uses., J.E. Casida and G.B. Quistad, eds (New York: Oxford University Press), pp. 123–193.

de Kraker, J.WFranssen, M.C., de Groot, AKonig, W.A., and Bouwmeester, H.J. (1998). (+)-Germacrene A biosynthesis. The committed step in the biosynthesis of bitter sesquiterpene lactones in chicory. Plant Physiol. **117:** 1381–1392.

Dickinson, C.M. (1982). Stability of individual natural pyrethrins in solution after separation by preparative high-performance liquid-chromatography. J. Assoc. Off. Anal. Chem. **65:** 921–926.

Doskotch, R.W., and Elferaly, F.S. (1969). Isolation and characterization of (+)-sesamin and beta-cyclopyrethrosin from pyrethrum flowers. Can. J. Chem. **47:** 1139.

Doskotch, R.W., Elferaly, F.S., and Hufford, C.D. (1971). Sesquiterpene lactones from pyrethrum flowers. Can. J. Chem. **49:** 2103.

Duke, M.V., Paul, R.N., Elsohly, H.N., Sturtz, G., and Duke, S.O. (1994). Localization of artemisinin and artemisitene in foliar tissues of glanded and glandless biotypes of *Artemisia annua* L. Int. J. Plant Sci. **155:** 365–372.

Duke, S.O., and Paul, R.N. (1993). Development and fine-structure of the glandular trichomes of *Artemisia annua* L. Int. J. Plant Sci. **154:** 107–118.

Duke, S.O., Vaughn, K.C., Croom, E.M., and Elsohly, H.N. (1987). Artemisinin, a constituent of annual wormwood (*Artemisia annua*), is a selective phytotoxin. Weed Sci. **35:** 499–505.

Elger, A., Lemoine, D.G., Fenner, M., and Hanley, M.E. (2009). Plant ontogeny and chemical defence: Older seedlings are better defended. Oikos **118:** 767–773.

Elliott, M. (1964). Pyrethrins and related compounds 3. Thermal isomerization of cis-pyrethrolone and its derivatives. J. Chem. Soc. 888.

Fahn, A. (2000). Structure and function of secretory cells. Adv. Bot. Res. **31:** 37–75.

Goldberg, A.A., Head, S., and Johnston, P. (1965). Action of heat on pyrethrum extract: The isomerisation of pyrethrins to isopyrethrins. J. Sci. Food Agric. **16:** 43.

Goodger, J.Q.D., Capon, R.J., and Woodrow, I.E. (2002). Cyanogenic polymorphism in *Eucalyptus polyanthemos* Schauer subsp. *vestita* L. Johnson and K. Hill (Myrtaceae). Biochem. Syst. Ecol. **30:** 617–630.

Göpfert, J.C., Heil, N., Conrad, J., and Spring, O. (2005). Cytological development and sesquiterpene lactone secretion in capitate glandular trichomes of sunflower. Plant Biol (Stuttg) **7:** 148–155.

Goren, N., Tahtasakai, E., Pezzuto, J.M., Cordell, G.A., Schwarz, B., and Proksch, P. (1994). Sesquiterpene lactones from *Tanacetum argenteum*. Phytochemistry **36:** 389–392.

Hanley, M.E., and Lamont, B.B. (2001). Herbivory, serotiny and seedling defence in Western Australian Proteaceae. Oecologia **126:** 409–417.

He, Z.Y., Li, L.G., and Luan, S. (2004). Immunophilins and parvulins. Superfamily of peptidyl prolyl isomerases in Arabidopsis. Plant Physiol. **134:** 1248–1267.

Head, S.W. (1966). A study of the insecticidal constituents in *Chrysanthemum cinerariaefolium*. (1) Their development in the flower head. (2) Their distribution in the plant. Pyrethrum Post **8:** 32–37.

Heinrich, G., Pfeifhofer, H.W., Stabentheiner, E., and Sawidis, T. (2002). Glandular hairs of *Sigesbeckia jorullensis* Kunth (Asteraceae): Morphology, histochemistry and composition of essential oil. Ann. Bot. (Lond.) **89:** 459–469.

Hemmerlin, A., Rivera, S.B., Erickson, H.K., and Poulter, C.D. (2003). Enzymes encoded by the farnesyl diphosphate synthase gene family in the Big Sagebrush *Artemisia tridentata* ssp. *spiciformis*. J. Biol. Chem. **278:** 32132–32140.

Iino, Y., Tanaka, A., and Yamashit, K. (1972). Plant-growth inhibitors 1. Plant-growth inhibitory activities of synthetic α-methylene-gamma-butyrolactones. Agric. Biol. Chem. **36:** 2505–2509.

Johnson, K.S. (1999). Comparative detoxification of plant (*Magnolia virginiana*) allelochemicals by generalist and specialist *Saturniid* silkmoths. J. Chem. Ecol. **25:** 253–269.

Kikuta, Y., Ueda, H., Takahashi, M., Mitsumori, T., Yamada, G., Sakamori, K., Takeda, K., Furutani, S., Nakayama, K., Katsuda, Y., Hatanaka, A., and Matsuda, K. (2012). Identification and characterization of a GDSL lipase-like protein that catalyzes the ester-forming reaction for pyrethrin biosynthesis in *Tanacetum cinerariifolium*– A new target for plant protection. Plant J. **71:** 183–193.

Krieger, R.I., Feeny, P.P., and Wilkinson, C.F. (1971). Detoxication enzymes in the guts of caterpillars: An evolutionary answer to plant defenses? Science **172:** 579–581.

Kumar, A., Singh, S.P., and Bhakuni, R.S. (2005). Secondary metabolites of Chrysanthemum genus and their biological activities. Curr. Sci. **89:** 1489–1501.

Kutchan, T.M. (2005). A role for intra- and intercellular translocation in natural product biosynthesis. Curr. Opin. Plant Biol. **8:** 292–300.

Li, J., Yin, L.Y., Jongsma, M.A., and Wang, C.Y. (2011). Effects of light, hydropriming and abiotic stress on seed germination, and shoot and root growth of pyrethrum (*Tanacetum cinerariifolium*). Ind. Crops Prod. **34:** 1543–1549.

Livak, K.J., and Schmittgen, T.D. (2001). Analysis of relative gene expression data using real-time quantitative PCR and the 2(-Δ Δ C(T)) method. Methods **25:** 402–408.

Maciver, D.R. (1995). Constituents of pyrethrum extract. In Pyrethrum Flowers: Production, Chemistry, Toxicology, and Uses, J.E. Casida and G.B. Quistad, eds (New York: Oxford University Press), pp. 108–122.

Matsuda, K., Kikuta, Y., Haba, A., Nakayama, K., Katsuda, Y., Hatanaka, A., and Komai, K. (2005). Biosynthesis of pyrethrin I in seedlings of *Chrysanthemum cinerariaefolium*. Phytochemistry **66:** 1529–1535.

Mullin, C.A., Alfatafta, A.A., Harman, J.L., Everett, S.L., and Serino, A.A. (1991). Feeding and toxic effects of floral sesquiterpene lactones, diterpenes, and phenolics from sunflower (*Helianthus annuus* L.) on western corn-rootworm. J. Agric. Food Chem. **39:** 2293–2299.

Nour-Eldin, H.H., and Halkier, B.A. (2009). Piecing together the transport pathway of aliphatic glucosinolates. Phytochem. Rev. **8:** 53–67.

Olofsson, L., Lundgren, A., and Brodelius, P.E. (2012). Trichome isolation with and without fixation using laser microdissection and pressure catapulting followed by RNA amplification: Expression of genes of terpene metabolism in apical and sub-apical trichome cells of *Artemisia annua* L. Plant Sci. **183:** 9–13.

Olsson, M.E., Olofsson, L.M., Lindahl, A.L., Lundgren, A., Brodelius, M., and Brodelius, P.E. (2009). Localization of enzymes of artemisinin biosynthesis to the apical cells of glandular secretory trichomes of *Artemisia annua* L. Phytochemistry **70:** 1123–1128.

Picman, A.K. (1983). Anti-fungal activity of helenin and isohelenin. Biochem. Syst. Ecol. **11:** 183–186.

Picman, A.K., and Towers, G.H.N. (1983). Anti-bacterial activity of sesquiterpene lactones. Biochem. Syst. Ecol. **11:** 321–327.

Pieper, G.R., and Rappaport, N.L. (1982). Photostabilization of bioethanomethrin, resmethrin, and natural pyrethrins (Pyrethrum) by mixed diaryl-para-phenylenediamines. J. Agric. Food Chem. **30:** 405–407.

Ratzka, A., Vogel, H., Kliebenstein, D.J., Mitchell-Olds, T., and Kroymann, J. (2002). Disarming the mustard oil bomb. Proc. Natl. Acad. Sci. USA **99:** 11223–11228.

Rivera, S.B., Swedlund, B.D., King, G.J., Bell, R.N., Hussey, C.E., Jr., Shattuck-Eidens, D.M., Wrobel, W.M., Peiser, G.D., and Poulter, C.D. (2001). Chrysanthemyl diphosphate synthase: Isolation of the gene and characterization of the recombinant non-head-to-tail monoterpene synthase from *Chrysanthemum cinerariaefolium*. Proc. Natl. Acad. Sci. USA **98:** 4373–4378.

Sashida, Y., Nakata, H., Shimomura, H., and Kagaya, M. (1983). Sesquiterpene lactones from pyrethrum flowers. Phytochemistry **22:** 1219–1222.

Schaffner, U., Vrieling, K., and van der Meijden, E. (2003). Pyrrolizidine alkaloid content in Senecio: Ontogeny and developmental constraints. Chemoecology **13:** 39–46.

Seaman, F.C., Fischer, N.H., and Stuessy, T.F. (1980). Systematic implications of sesquiterpene lactones in the subtribe Melampodiinae. Biochem. Syst. Ecol. **8:** 263–271.

Susurluk, H., Caliskan, Z., Gurkan, O., Kirmizigul, S., and Goren, N. (2007). Antifeedant activity of some *Tanacetum* species and bioassay guided isolation of the secondary metabolites of *Tanacetum cadmeum ssp cadmeum* (Compositae). Ind. Crops Prod. **26:** 220–228.

Thulasiram, H.V., Erickson, H.K., and Poulter, C.D. (2007). Chimeras of two isoprenoid synthases catalyze all four coupling reactions in isoprenoid biosynthesis. Science **316:** 73–76.

Werker, E. (2000). Trichome diversity and development. Adv. Bot. Res. **31:** 1–35.

Yang, T., Stoopen, G., Wiegers, G., Mao, J., Wang, C.Y., Dicke, M., and Jongsma, M.A. (2012). Pyrethrins protect pyrethrum leaves against attack by western flower thrips, *Frankliniella occidentalis*. J. Chem. Ecol. **38:** 370–377.

Zito, S.W., Zieg, R.G., and Staba, E.J. (1983). Distribution of pyrethrins in oil glands and leaf tissue of *Chrysanthemum cinerariaefolium*. Planta Med. **47:** 205–207.